Composites Part B 77 (2015) 462–473

Contents lists available at ScienceDirect

Composites Part B

journal homepage: www.elsevier.com/locate/compositesb

# An experimental investigation into quasi-static and fatigue damage development in bolted-hole specimens

O.J. Nixon-Pearson*, S.R. Hallett

*University of Bristol, Advanced Composites Centre for Innovation and Science, Queens Building, University Walk, Bristol BS8 1TR, UK*

ARTICLE INFO

*Article history:*
Received 12 November 2014
Received in revised form
4 March 2015
Accepted 16 March 2015
Available online 23 March 2015

*Keywords:*
A. Carbon fibre
B. Delamination
B. Fatigue
D. X-ray computed tomography (CT)

ABSTRACT

An extensive experimental program has been carried out to investigate and understand the sequence of damage development throughout the life of bolted-hole composite laminates under quasi-static loading and tension–tension fatigue. Quasi-isotropic carbon/epoxy laminates, with stacking sequence $[45_2/90_2/-45_2/0_2]_S$ defined as ply scaled and $[45/90/-45/0]_{2S}$ defined as sub-laminate scaled, were used. Specimens were cycled at 5 Hz with various amplitudes to $1 \times 10^6$ cycles unless failure occurred prior to this limit. For all cases an R ratio of 0.1 was used. Bolt washer pressures of 23 MPa and 70 MPa were investigated. For the ply-level case, the quasi-static test showed both delamination and fibre-dominated pull-out failures for a washer pressure of 23 MPa, and pull-out failure only for 70 MPa. Delamination dominates in fatigue tests. For the sub-laminate case the tests failed by pull-out in both quasi-static and fatigue tests for all washer pressures. It is shown in this paper how the role of delamination is critical in the case of fatigue loading and how this interacts with bolt clamp-up forces. A number of tests were analysed for damage using X-ray CT scanning and comparisons of damage are made with tests from previous open-hole studies.



## 1. Introduction

Fibre-reinforced composites laminates are increasingly being used to manufacture load bearing primary structures in the aerospace sector as composites offer a much better strength to weight ratio than metals. Joints which use fasteners are very commonplace in the assembly of aircraft structures. The complex failure modes of composites materials and the requirement for fasteners however demand a more rigorous approach to design than for traditional alloys. Bolt filled-hole, along with open-hole tension tests are widely used in industry to aid the understanding of the behaviour of the tensile strength of bolted joints.

Factors affecting the characteristics of open and filled-hole laminate strengths include, ply orientation, washer pressures and washer sizes. There is still rather limited understanding of the mechanisms and causes of the differences in failure strength between the filled-hole and open-hole specimens. Previous work in this area includes an experimental study carried out to investigate the effects of clamp-up on the net-tension (quasi-static) failure of composite plates with bolt filled-holes by Yan et al. [1]. Bolted joints (100% bolt bearing load) and non-bolt bearing load (100% bypass tensile load) conditions were investigated. For bolted joints which failed in a net-tension mode, the bolt clamping force increased the strength of the joint irrespective of the layup. There have also been other quantitative studies into the tensile strength and fatigue behaviour of bolted composite joints with single and multiple numbers of bolts [2–4].

Persson and Eriksson [3], for example, investigated various different conditions of multiple row bolted joints to include geometry (width, spacing, and edge distances), laminate configuration, fastener type, and environmental conditions. They found that the most significant factors were the ratio of bolt diameter to specimen width, and the ratio of hole diameter to laminate thickness when using single-lap joints containing four fasteners and two rows. However very little work is available in the literature on the interactions between the sub-critical damage and the bolt clamp-up forces.

Previous work has investigated open-hole tension damage mechanisms in detail under static loading [5] and fatigue [6–8]. These studies found that delamination plays a significant role in cases with thick ply blocks, where the hole diameter to ply block thickness ratio is relatively small. This results in increasing failure

* Corresponding author.
*E-mail address:* on5405@bristol.ac.uk (O.J. Nixon-Pearson).

http://dx.doi.org/10.1016/j.compositesb.2015.03.051

stresses for increasing in-plane dimensions using constant thicknesses. In contrast for cases with dispersed plies and repeated sublaminates through the thickness the reduction in the amount of damage propagating through the gauge section for configurations with larger hole-diameters means that there is a reduced amount of stress relief at the hole-edge, leading to earlier fibre-dominated failure. The effect of out of plane compressive stress on enhancing delamination strength is well known in composites [2]. It is thus expected that when the same configurations as tested in open-hole tension are subject to bolt clamping forces, this will have a direct effect on the damage formation and hence ultimate strength.

Since the understanding of formation and propagation of damage is of great importance to the overall failure of open-hole tension specimens, particularly in fatigue, this was investigated and characterised using X-ray Computed Tomography (CT) scanning in Refs. [6,8]. In other earlier fatigue related work, Spearing and Beaumont [9] concentrated on tension–tension fatigue of notched Carbon/Epoxy (T300/914) and Carbon/Polyetheretherketone (PEEK) laminates using an R ratio of 0.1. NDT (non-destructive testing) techniques included X-radiography to produce images of the damage. It was also shown how prolonged exposure to the zinc iodide dye penetrant can accelerate the growth of damage in the specimens. Other early work was carried out by Mohlin et al. [10,11] using tetrabromoethane (TBE) enhanced X-ray radiography to study delamination growth in notched/carbon epoxy laminates under compressive fatigue loading. The main limitations of this early work is the 2D nature of damage characterisation, and the inability to separate out the global damage into individual delamination interfaces and ply cracking orientations. Fatigue damage in composites is distinctly three dimensional in character and therefore more recent techniques such as X-ray computed tomography (CT) are much more suitable for the evaluation of the micromechanical behaviour of fatigue damage development. Work by Scott et al. [12] and Moffat et al. [13] has proven the capability of this technique to identify damage progression in notched carbon-epoxy specimens under quasi-static loading to failure.

In this paper the role of bolted clamp-up forces is examined in regard to its effect on the formation of damage in bolted-hole tension tests both in static and fatigue. The damage is characterised through X-ray CT scanning of tests interrupted at various stages of the damage formation and results are compared against previous open-hole tension fatigue work [6,8,14].

## 2. Experimental procedure

The material used is Hexcel's carbon fibre-epoxy unidirectional (UD) prepreg system, IM7/8552, with a nominal ply thickness of 0.125 mm [15]. The specimen dimensions are shown in Fig. 1. Holes were drilled using a brad-point (also known as lip and spur), tungsten carbide drill bits. The lip and spur (also known as the brad point) drill bit, is optimised for drilling wood. Conventional drill bits may wander prior to initial contact with a flat surface, the sharp point of the spur pushes into the material keeping it in line. When drilling wood across the grain there is a tendency for the long fibres to pull-out around the circumference of the hole-edge rather than being cleanly cut. This also applies to composite materials which like wood contains many fibres. The lip and spur drill bit cuts the outer periphery of the hole prior to the inner cutting edges, planing the base of the hole. Thus the lip ensures that the fibres at the hole-edge are cut cleanly rather than pulling them out and splintering them.

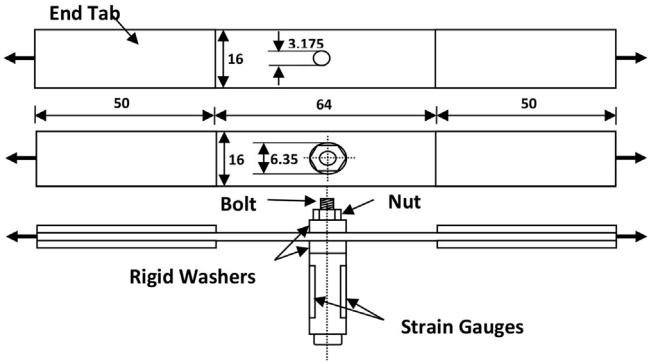


**Fig. 1.** Open and bolted hole specimen dimensions.

Drilling parameters used in this paper were 1500 rpm (spindle speed), with a feed rate of 1 mm/min. If drill speed is too high then the propensity to generate heat is increased, if too low then the risk of back face delamination damage is enhanced. The specimen was clamped to a back plate in order to minimise back-face breakout. The drilling method used here is consistent with previous open-hole quasi-static and fatigue work carried out by the authors [6,8].

Quasi-static open-hole tests carried out by Green et al. [5] used reamed holes when preparing specimens of the same configuration. X-ray images in Ref. [16] show minimal damage in areas not affected by mechanical loading. X-ray images in Refs. [6,8] show similar low levels of drilling damage and more importantly, close agreement was obtained between the quasi-static tensile results from Ref. [5] and those obtained in Refs. [6,8], thus indicating that hole drilling quality was sufficient so as not to influence the results.

The ratio of width to hole diameter chosen represents the minimum distance needed to allow the elastic stress states to return sufficiently close to their original values at the edges, thereby giving dimensions offering the lowest failure forces, and using the least amount of material. The geometry used here had a W/d ratio of 5 to ensure consistency with previous extensive work on open-hole tensile specimens [5–8], which was based on an industrial test standard. This is slightly lower than the recommended W/d ratio of 6 in the ASTM D6742 standard.

In order to measure the clamping stress around the hole, a bush made from 6082-T6 aluminium alloy, with strain gauges bonded at opposite sides was used. These were calibrated so as to accurately calculate the clamping stresses and to ensure that there was no bending of the bush. Two “rigid” 4 mm thick aluminium washers of diameter 6.35 mm were then placed adjacent to the composite (Fig. 1) to apply the contact load. This gives a washer diameter to hole diameter ratio of 2:1. A4 class 70 stainless steel M3 bolts were used, with a measured thread diameter of 2.95 mm (using digital Vernier callipers). The hole diameter of the specimens was 3.175 mm (1/8 inch), thus the bolt thread diameter is a clearance fit with respect to the specimen holes so as to eliminate contact stress at the hole edge as an experimental variable.

The hole-diameter of the washer and bush is 3.1 mm with a maximum allowable shift of 0.15 mm with respect to the bolt. Care was taken when tightening to ensure that the washer remained central with the hole.

Quasi-isotropic carbon/epoxy laminates, with stacking sequence $[45_2/90_2/\text{-}45_2/0_2]_S$ and $[45/90/\text{-}45/0]_{2S}$ were used. The first, with plies blocked together is termed ‘ply-level scaled’, and the second, with repeated sub-laminate units is termed ‘sub-laminate-level scaled’. The load bearing plies in the 0° direction are not at the surface and are thus more protected from impact damage, which is consistent with standard industry practice. These configurations were chosen as the open-hole ply-level specimens exhibited delamination dominated failure in quasi-static testing, with sub-laminate level specimens showing a fibre dominated pull-

out type failure [5]. Bolt pressures of 23 MPa and 70 MPa were used for quasi-static testing, with 70 MPa used in fatigue, as the greater out-of-plane stresses are likely to produce the most notable effects. These bolt pressures were chosen from Ref. [1] as they represent pressures which gave the most notable effects for similar configurations. Tightening torque can be estimated from equation (1):-

$$T = K \cdot d \cdot F_{bolt} \tag{1}$$

where T is the torque applied, K is the "nut factor" for which a typical value of 0.2 is used, d is the bolt diameter and $F_{bolt}$ is the axial bolt force. From the washer pressure and area the bolt force can be calculated as 554.8 N and 1688.4 N for the 23 and 70 MPa respectively, giving a tightening torque of 0.327 and 0.996 Nm. These values were low enough to be torque tightened using a hand-held hex key.

Using the bolt nominal stress area of 5.03 $mm^2$ the bolt stresses can be calculated to be 110.3 MPa and 335.7 MPa for the 23 and 70 MPa cases, well below the bolt yield stress of 450 MPa. Five quasi-static tests were carried out for each layup and washer pressure using a crosshead speed of 1 mm/min in all cases. The fatigue tests were run at various percentages of the average static failure load. Fatigue tests were run in load control at constant amplitude, with an R ratio of 0.1 and a frequency of 5 Hz. Each test was run to $10^6$ cycles unless failure (defined as a 15% loss of stiffness) occurred prior to reaching this limit. This failure criterion was chosen by the authors and used in previous work [6,8] as it consistently represents the level of stiffness loss that corresponds to the change to an almost vertical slope in the stiffness versus number of cycles-curve.

$10^6$ cycles is commonly used in the aerospace industry as appropriate for the number of load cycles experienced during the useful life of an aircraft [17]. Fatigue tests have previously been carried out at 40%, 50%, 60%, 70% and 80% of the nominal static failure load $P_{max}$ for ply level open-hole tests [6], and here 50%, 60%, 70% and 80% severities for bolt-filled ply-level specimens are used. For sub-laminate specimens, open-hole tests previously used 55%, 60%, 65%, 70% 80%, 85% and 90% of static failure load, and here 80%, 85% and 90% severities have been used for the bolt-filled sub-laminate-level specimens. To characterise the effect of damage propagating under fatigue from the hole and free edge, an effective stiffness, $E_{eff}$, is calculated by using equation (2) below [6,8]:

$$\boldsymbol{E_{eff}} = \frac{(\boldsymbol{P_{max}} - \boldsymbol{P_{min}})}{\boldsymbol{A}(\varepsilon_{\boldsymbol{max}} - \varepsilon_{\boldsymbol{min}})} \approx \frac{\boldsymbol{P_{max}}}{\boldsymbol{A}(\varepsilon_{\boldsymbol{max}} - \varepsilon_{\boldsymbol{min}})} \tag{2}$$

where $P_{max}$ is the load at peak amplitude, $P_{min}$ is the load at the trough, A as the gross cross sectional area of the specimens and $\varepsilon$ is the strain measured using a clip gauge extensometer recorded over a gauge length of 50 mm, symmetric about the hole for each specimen. The clip gauge and the relative stiffness change is used to identify the point of critical propagation of damage. The absolute value of stiffness is thus not of great significance, it is the normalised relative stiffness that is more important in the construction of the S–N curves.

The quasi-static and fatigue damage of selected bolted hole specimens were analysed using X-ray CT and compared to previous work on the damage behaviour of open-hole specimens [6].

### 2.1. NDT: 3D X-ray computed tomography

X-ray CT is rapidly becoming an increasingly important tool in the micromechanical damage analysis of materials [18] enabling routine non-destructive 3D imaging in the micron range.

To enhance X-ray contrast these samples were soaked in X-ray dye penetrant comprising 250 g zinc iodide, 80 ml distilled water, 80 ml isopropyl alcohol and 1 ml kodak photoflow, over a period of 2 days. Zinc iodide was used because it is relatively non-toxic and is reasonably X-ray opaque.

Micro X-ray CT scanning was performed at the UK National Composites Centre (NCC) in Bristol using a Nikon XT H 225 kV electron beam machine. Each specimen is mounted on the rotation stage and positioned between the X-ray source and the 2000 × 2000 16 bit pixel panel detector. A cone of X-rays is emitted from the target and passes through the specimen to the detector. During the scan, the specimen is incrementally rotated through 360° about the Z-axis with an X-ray image radiograph (projection) collected at each orientation. The individual set of radiograph projections are reconstructed into a 3D volume using a filtered back-projection reconstruction algorithm. For successful reconstructions, the width of the specimen (i.e. the dimension normal to the rotation axis) must always lie within the X-ray cone as it is rotated. The scanning voltage was 80 kV (320 μA) and the exposure time for each radiograph was 250 ms. The Metris CT Pro software was used to reconstruct each scan volume with post-processing and analysis performed using the VG studio max 2.1 and Avizo® 7 software packages. This enables visualisation of the volumes of a given sample as a 3D map in which the grey scale value corresponds to the local X-ray absorption coefficient of the material. There are two peaks on the histogram of the grey scale intensity which indicates the solid material (fibres and matrix), and air (matrix cracking, delaminations, voids and other defects). Hence the matrix cracks and delaminations could be segmented by defining certain thresholds around the appropriated grey scale values [19].

For fatigue damage, a semi-automatic process was used for the analysis. A region of interest was placed around the approximate region of damage, if there was only localised damage in the specimen then a region close to the hole-edge was selected. For extensive delamination damage, a region of interest was selected to include the entire length of the specimen. A 3D seed growth tool was used in order to capture some excess damage which didn't absorb the penetrant and to be able to capture the damage with greater precision. This tool enables segmentation of voxels by addition of all the adjacent points of a defined seed point which are within a tolerance with respect to the mean grey value of the selection [12].

## 3. Quasi-static testing of bolted-hole specimens

The initial bolted ply-level static tests were carried out using specimens manufactured from the same plate as the third batch of open-hole specimens used in the fatigue work described in Ref. [6]. Likewise the initial bolted sublaminate static tests used some specimens from the same plate as the second batch of open-hole sublaminate-level fatigue specimens from Ref. [6]. Therefore the static open-hole strengths were already characterised and documented, allowing for a straightforward comparison for the bolted results. A fourth batch of ply-level specimens were produced, which was used to carry out further bolted hole static testing and subsequent fatigue testing. A static interrupted test was loaded to 80% of the failure strength of a ply-level bolted specimen from the fourth batch to observe any subcritical damage. Another batch of specimens was produced for the sublaminate-level bolted fatigue tests. Table 1 shows all quasi-static bolt-filled hole results and their corresponding failure mode. D denotes delamination failure, P denotes pull-out.

For the ply-level specimens (which have an open-hole failure mode by delamination) using a washer pressure of 23 MPa, an

**Table 1**
Summary of bolted results with their open-hole counterparts across all batches.

| Layup | Batch number | Washer pressure (MPa) | Strength, MPa (CV%) | Number of specimens tested | Failure mode |
|---|---|---|---|---|---|
| Ply-level | 3 | Open-hole | 395.7 (5.43%) | 4 | 4xD |
| Ply-level | 3 | 23 | 476.8 (4.4%) | 5 | 2xP, 3xD |
| Ply-level | 3 | 70 | 505.1 (2.9) | 5 | 5xP |
| Ply-level | 4 | 70 | 495.3 (4.5%) | 3 | 3xP |
| Sub-laminate | 2 | Open-hole | 531.8 (3.13%) | 4 | 4xP |
| Sub-laminate | 2 | 23 | 526.2 (2.0) | 5 | 5xP |
| Sub-laminate | 2 | 70 | 544.1 (3.1%) | 5 | 5xP |
| Sub-laminate | 3 | 70 | 561.3 (4.9%) | 3 | 3xP |

average failure strength of 476.8 MPa was recorded with a CV of 4.4%. This is remarkably higher than the open-hole strength of 395.7 MPa (with a CV of 5.4%) from the same batch of material, giving an increase in strength of 17.3%.Two of the five bolted specimens failed via pull-out, and three out of five specimens failed by delamination. For the ply-level specimens using a washer pressure of 70 MPa, an average failure strength of 505.1 MPa with a CV of 2.9% was recorded for 5 specimens. The next batch of specimens tested with the same 70 MPa washer pressure gave a failure strength of 495.3 MPa with a CV of 4.5% for 3 specimens. For the 70 MPa case pull-out failure occurred for all ply-level specimens tested. The batch 4 result was used to set the fatigue severities used in the following section.

Fig. 2 shows stress-crosshead displacement curves from three ply-level tensile tests; two for a washer stress of 23 MPa, one of which failed by pull-out and the other by delamination, and one for a washer stress of 70 MPa. The 23 MPa delamination case is an example of a test with load drops, due to the delamination occurring asymmetrically either side of the hole. After the first load drop, caused by delamination back to the grips, the load began to increase again until recovered to a similar level, when the second delamination propagated, causing the second load drop. After this the load increased again until fibre failure in the remaining 0° ligaments was observed. Although the specimens were loaded until failure of the 0° plies, the specimen had lost its structural integrity during the first major delamination, which is classed as the failure point. Applying a washer pressure around the hole-edge, increases the stresses required for delamination. There is thus a higher

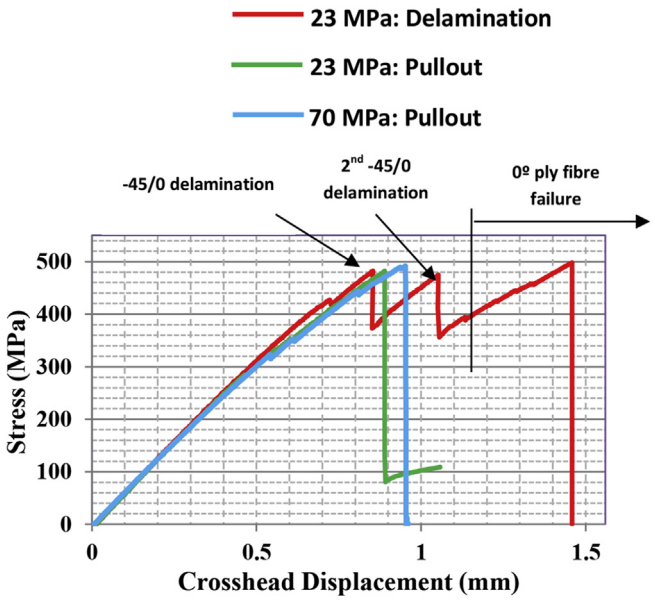


**Fig. 2.** Ply-level tests with a bolt-filled hole.

overall level of stress in the plies at the point at which delamination initiates compared to the open hole case. Once delamination starts to propagate it can happen that for some cases the load redistribution is sufficient to cause fibre failure, resulting the pull-out type failure. At this level of clamping pressure the specimens are thus in a transition regime between the two modes.

When the washer pressure is increased to 70 MPa the enhancement of the delamination stress is such that fibre failure stress is consistently reached prior to full width delamination and pull-out failure occurs in all cases. The load curve for these specimens, as shown in Fig. 2, is very similar to the 23 MPa pull-out case.

There are some small drops in load prior to failure, which is due to subcritical damage in the form of matrix cracks and small localised delaminations. This cumulatively adds to the non-linearity of the curve but the load drops are not large enough to exceed the static failure criterion of a 5% load drop. Readers are referred to references [5,16] for a more extensive discussion on the differences between the delamination and pull-out failure mechanisms. Fig. 3 shows some of the clearest examples of (a) pullout failure, and (b) delamination failure from the open-hole tensile strength scaling study in Ref. [5].

Fig. 4 shows X-ray CT scans of a ply-level 70 MPa washer pressure test loaded quasi-statically to 80% of the failure strength and then interrupted. Each image in the table shows the respective plies through the laminate thickness on one side of the center-line for a single specimen, along with an image of all of the damage at every interface. In some plies there is some “shadowing” from the adjacent interfaces due to the minimum resolution that could be obtained from the CT scans. The damage is mostly in the form of extensive matrix cracks in the surface 45° and 90° plies, which are dispersed throughout the entire length of the specimen. There is very little damage in the −45° and 0° plies with no observable delaminations. This differed substantially from the equivalent open-hole test which is also included in Fig. 4 where the matrix splits were only observed local to the hole at 80% of the failure load [6]. When comparing the magnitude of the peak loads of the bolted hole specimens at 80% severity ($0.8 \times 505$ MPa $= 404$ MPa) to the open-hole strength of 395 MPa it is clear that the interrupted load of the bolted specimen is greater than the failure strength of the open-hole specimens. A greater amount of matrix cracking therefore occurs than was observed in the ply-level open-hole static interrupted test at 80% $\sigma_{UTS}$ [6].

The failure strengths of the bolt filled sublaminate specimens using a washer pressure of 23 MPa were found to be 526.2 MPa with a CV of 2.0%, and for the washer pressure of 70 MPa, 544.1 MPa with a CV of 3.1% for 5 specimens in each case. A new batch of sublaminate level specimens (batch number 3) was manufactured for fatigue testing using a washer pressure of 70 MPa only. The quasi-static failure strength for this batch was 561.3 MPa with a CV of 4.9% over three specimens using a washer pressure of 70 MPa. This result was used to set the severity for fatigue tests where only the 70 MPa washer pressure is used.

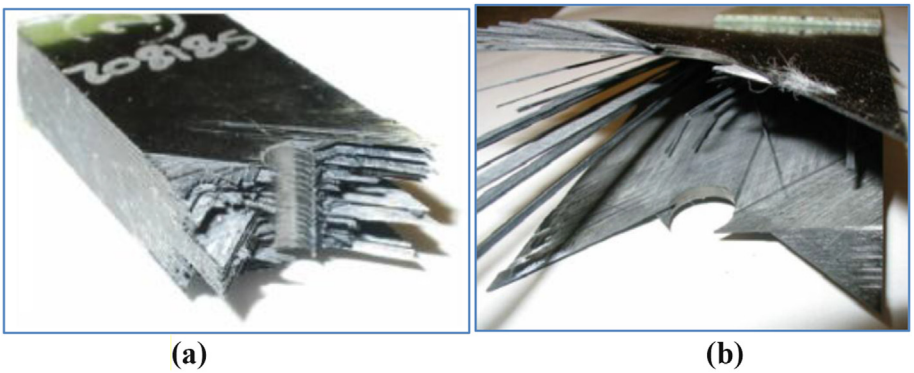


**Fig. 3.** Examples of pullout failure: (a), and delamination failure: (b) from Ref. [5].

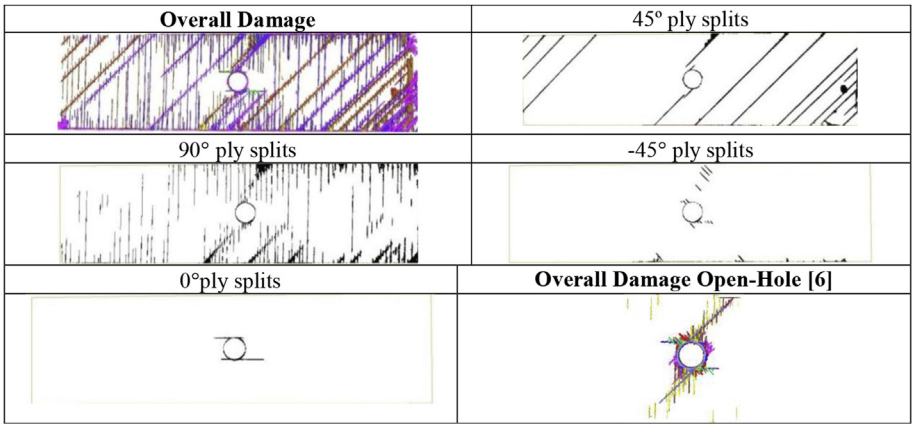


**Fig. 4.** CT images of a static ply-level interrupted test at 80% strength for washer pressure of 70 MPa compared with the equivalent open-hole test.

For bolt-filled hole sublaminate tests at both washer pressures, there was very little difference from the open-hole strength of 531.8 MPa with a CV of 3.13%. All specimens for both washer pressures failed by pullout as per the open-hole case. Fig. 5 shows an example of the typical stress displacement curve as well as variation of the washer pressures on the secondary axis for a bolted-hole static test at 70 MPa. Typically the strains on each side of the bush (washer pressures) are no more than 5% apart. As the load increases up to failure the washer pressures decreases slightly due to Poisson's contraction of the specimen. When the specimens fail, a small abrupt decrease in the washer pressure is observed as the damage causes the properties of the material below the washer to degrade.

A statically loaded test was interrupted at 90% of the failure strength for the sub-laminate level bolted-hole specimen using a 70 MPa washer pressure. There was very little sub-critical damage observed (Fig. 6). The damage was mostly small matrix splits in the 90° plies around the hole-edge and also the edges of the specimen. The open-hole equivalent showed a very similar level of damage.

To summarise, only if the laminates are prone to failure by delamination, does the static failure strength increase. The bar chart in Fig. 7 shows the effect of the bolt-filled holes and clamping pressure compared to that of the open-hole configuration. The figure shows that the greatest increase in the failure strength occurs for the ply-level specimens when the washer pressure is first introduced at 23 MPa. The failure strength is now much closer to the strengths of the sublaminate configurations. Inhibiting the delaminations by using a clamping pressure increases the stresses required for delamination to the point at which pull-out failure is consistently observed. The sublaminate configuration was least

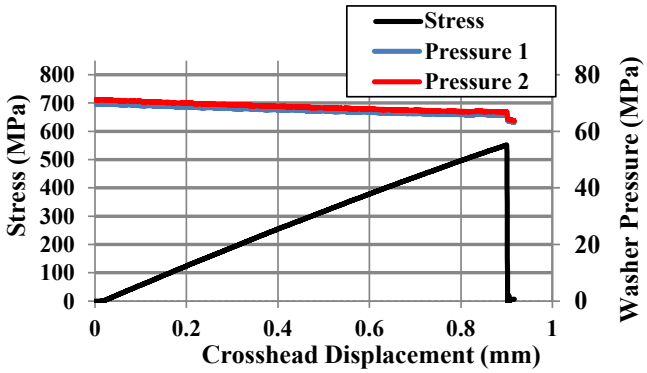


**Fig. 5.** An example of a sublaminate-level test with a bolt-filled hole and washer pressure of 70 MPa.

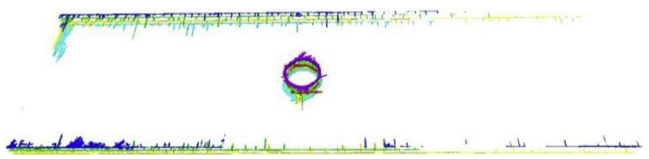

**Fig. 6.** Sub-critical damage in a bolted quasi-static sublaminate test interrupted at 90% strength.

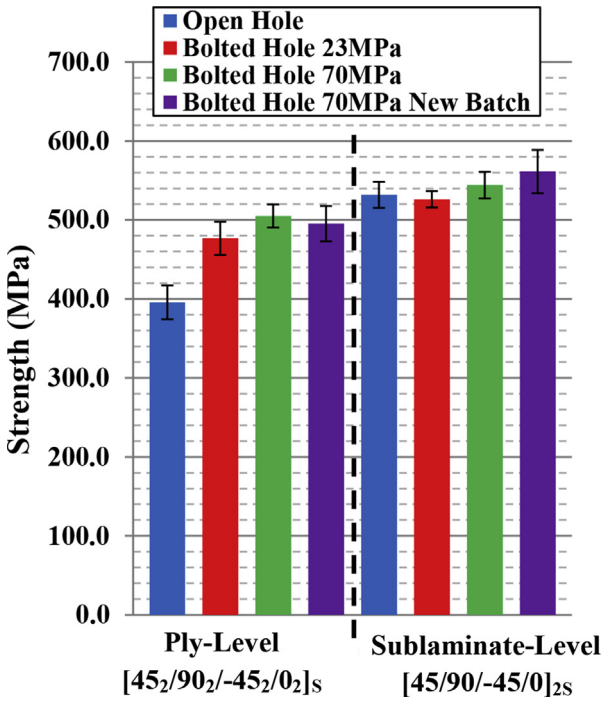


**Fig. 7.** Bar chart for all configurations for ply and sublaminate tests with their failure strengths.

affected by the bolt clamp-up in terms of the failure strength and mode of failure in static tests, however this configuration had previously shown a failure mode change from pull-out to delamination in open-hole fatigue testing. It was thus of interest to test both cases in fatigue for the bolted configuration. Although the average sublaminate level quasi-static strength for 23 MPa washer pressure is slightly lower than the open-hole quasi-static strength, the scatter for both configurations is greater than the difference in the strengths and so in terms of statistical significance the results can be considered to be the same. For the 70 MPa washer pressure sublaminate configuration the batch to batch variation in the average strengths is greater than the difference from the open-hole quasi-static and 23 MPa washer pressure strengths. Thus no overall trend in the sublaminate level configuration results could be observed, unlike for the ply-level configuration, and it therefore can be concluded that the washer pressure has no measurable effect on the sublaminate quasi-static strengths.

## 4. Bolted hole fatigue testing

The bolted case was studied under fatigue loading to investigate possible differences due to the effects of clamp-up. For both the ply-level and sublaminate specimens the fatigue tests were carried out using a clamp-up pressure of 70 MPa only. From the quasi-static testing of the ply-level case this condition gave the most consistent change in failure mode from open hole to bolted testing. For the sublaminate case, although very little change was observed between the open hole and bolted condition in static tests it was postulated that if any differences were to be observed in fatigue, these would occur at the highest clamping pressure, minimising delamination initiation around the hole. Open-hole tension fatigue tests using ply-level specimens gave delamination as the dominant failure mode [6]. Sublaminate-level tests gave a change in failure mode from pull-out, in the static case, to delamination dominated failure in all but the highest of severities of fatigue loads. Currently there has been very little work carried out on the effects of clamp-up pressure under fatigue loading conditions. A new batch of ply and sublaminate-level specimens were needed for the fatigue study on the effects of a bolt clamp-up stress. The results for three static tests on the new batches of specimens showed excellent consistency with previous results. The Weibull distribution is commonly used in survival analysis, reliability engineering and in failure analysis [20]. The probability function of a Weibull random variable is shown in equation (3):

$$f(x;\alpha,\beta)=\begin{cases}\frac{\beta}{\alpha}\left(\frac{x}{\alpha}\right)^{\beta-1}e^{-\left(\frac{x}{\alpha}\right)^{\beta}}, & x\geq 0\\ 0, & x<0\end{cases} \tag{3}$$

where $\alpha$ is the scale parameter, $\beta$ is the shape parameter (also known as the Weibull modulus). The Weibull random variable, $x$, in this instance is the number of cycles $N_f$. The fit of data is assessed using a Weibull plot. Equation (3) is integrated to give the cumulative density function in Equation (4) which is rearranged to give (5).

$$P_x=1-e^{-\left(\frac{x}{\alpha}\right)^{\beta}} \tag{4}$$

$$1-P_x=e^{-\left(\frac{x}{\alpha}\right)^{\beta}} \tag{5}$$

$$R_x=1-P_x \tag{6}$$

The probability of failure is given by $P_x$, and the probability of survival is given by $R_x$ (6). Taking the natural logarithm of each side in equation (5) gives equation (7) in the linear regression form of $y=mx+c$ respectively, thus giving $N_f=\ln x$, $m=\beta$, and $c=-\beta\ln\alpha$.

$$\ln\left(\ln\left(\frac{1}{1-P_x}\right)\right)=\beta\ln(x)-\beta\ln(\alpha) \tag{7}$$

The method of obtaining Probability of survival vs number of cycles plots is as follows:

- For each fatigue severity or stress level, the number of cycles to failure must be known.
- For a given severity a serial number must be assigned to each failure value (i = 1, 2, 3 … ).
- Each value of failure probability used the Bernard's Median Rank formula defined in equation (8):

$$MR=\frac{i-0.3}{n+0.4} \tag{8}$$

where i is the serial number assigned to a failure within a particular fatigue severity, and n corresponds to the number of specimens in the given severity.

- Values for $ln(\ln(1-MR))$, and $\ln(N_f)$ were calculated, and plotted on y and x axes respectively, in order to obtain parameters á and â via linear regression analysis (omitted here for simplification).
- Once parameters á and â are known, equation (9) is used for the calculation of life for a given probability of failure as shown in Figs. 9a, b, and 16a, b.

$$N_{R_x}=\alpha\cdot(-ln\,R_x)^{1/\beta} \tag{9}$$

For further details of other successful applications of Weibull statistics to fatigue data see Ref. [20]. The main advantages of using a Weibull analysis is its ease of application due to simple functions. It also provides some aid to physical rules regarding failure. The disadvantages of using this method are that it becomes more unreliable with smaller sample sizes and with specimens that fail in different modes, as in this paper. The ASTM E739-10 standard [21] gives reasonable guidelines for the minimum sample sizes required for a given test. The sample sizes in this paper are representative of preliminary and exploratory coupon level experiments (sample sizes ranging from 3 to 11 specimens depending on severity and configuration). Design allowables and reliability data typically require sample sizes between 12 and 24 specimens.

### 4.1. Bolt-filled hole ply-level results

A minimum of 3 specimens were tested at 80%, 70% and 60% severity with a single run-out test at 50% severity. The results show a significant increase in the number of cycles to failure for the severities tested in comparison to the open-hole specimens. Fig. 8 shows a clear shift in the SN curve, giving failure at a higher number of cycles for a given severity for the bolted case. Fig. 9(a) and (b) show the Weibull distribution for open- and bolted-hole ply level specimens respectively. The plots show a good fit for the open-hole data which contains a wide enough sample size for accurate Weibull analyses with reasonable fits for bolted specimens.

This is due to the clamp-up pressure which delays the onset of delamination from the hole-edge. For the majority of the bolted specimens with the ply-level configuration, once damage starts to propagate there is an initial decrease in the stiffness which satisfies the failure criterion, but the effective modulus curve then levels out at a plateau at approximately half way through the total stiffness decrease (Fig. 10). This can be attributed to the clamp-up pressure which inhibits the propagation of the 2nd asymmetric delamination of the -45/0 interface. There are some delaminations initiating from the specimen edges. Fig. 10 shows the fatigue results for selected ply-level bolted-hole cases which are representative stiffness loss curves, including some of the samples that were CT scanned.

In the specimen naming convention, B denotes that the specimen is bolted, this is followed by the test number and severity. All specimens tested failed by delamination at the 15% stiffness drop threshold.

In the case of specimen B007-70%, this failed in a similar manner to the open-hole ply-level specimens but after delamination has occurred fibre-failure ensues at the second plateau when only the

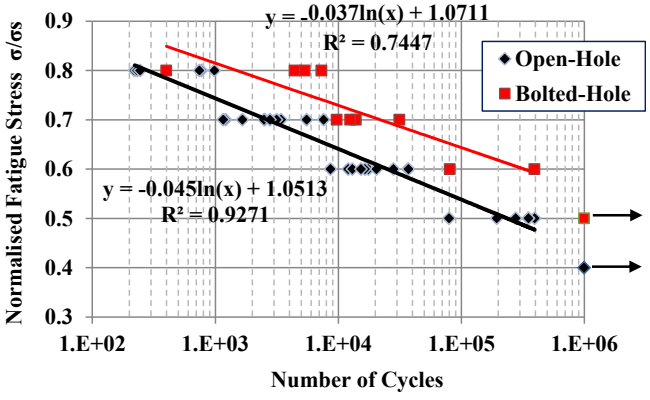


**Fig. 8.** The relationship between open-hole and bolted-hole in fatigue loading for ply-level specimens.

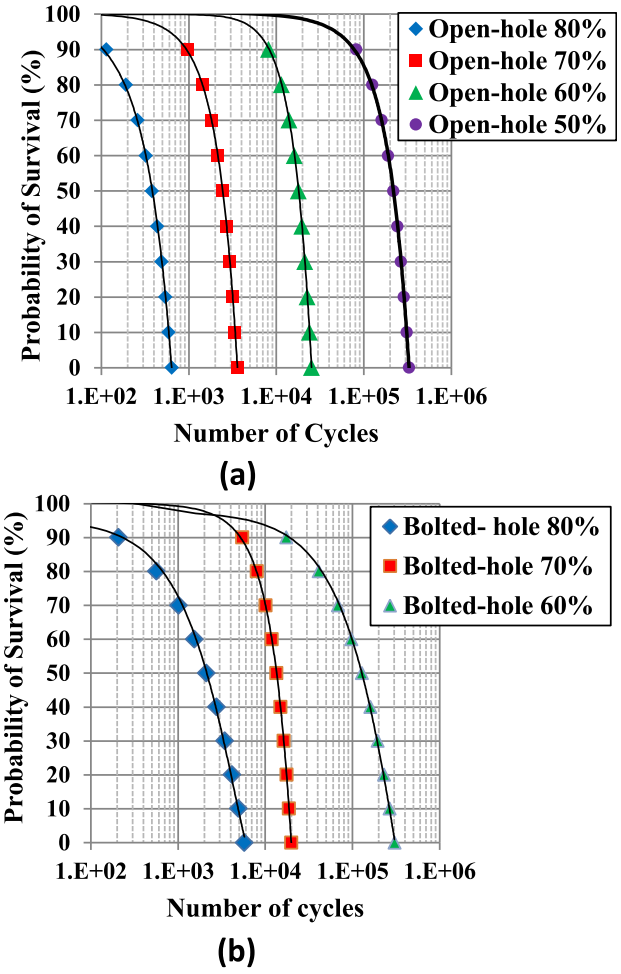


**Fig. 9.** Probability of survival graphs for ply-level (a) open- and (b) bolted-hole test programmes.

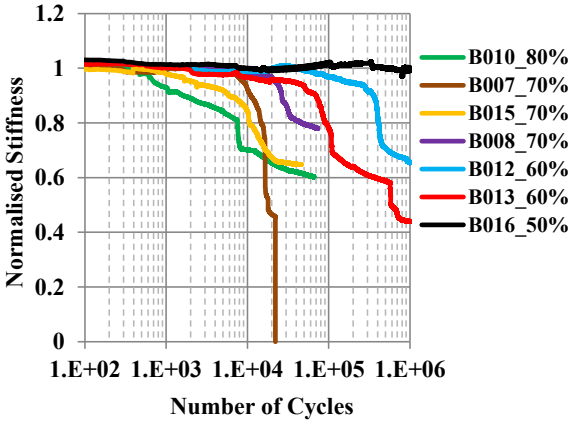


**Fig. 10.** Initial results obtained for the bolted ply-level fatigue tests.

0° plies are carrying the load. This phenomenon was commonly observed in the open-hole sublaminate fatigue tests, but never in the ply-level open-hole cases, where the second plateau is continuous without any fibre failure.

In all but the test case of specimen B007-70%, the stiffness decreases from the initial plateau and levels out at a normalised

stiffness of around $E/E_0 = 0.7$. The second drop in the stiffness occurs after a sizable delay, as seen in specimen B013 at 60% severity. To get a better understanding of the damage, specimen B012 and B013 (60% severity tests) were analysed by X-ray CT. Specimen B012 reached $10^6$ cycles whilst still on the first plateau (normalised stiffness of ~0.7) when the test was stopped at $10^6$ cycles. Specimen B013, tested at the same severity by contrast had reached the second plateau (normalised stiffness of ~0.5) after the same number of cycles. Fig. 11 shows the extent of the damage in specimen B012. This epitomises the damage seen in all specimens at $E/E_0 = 0.7$.

Fig. 12 shows the completely damaged specimen B013 at 60% severity. Firstly it is notable that the bolted −hole fatigue damage differs somewhat from open-hole fatigue tests. There is significant edge delamination in the 90/-45 interface due to the surface plies being more constrained around the hole by the bolt clamping force thus delamination can't open up so easily, causing them to initiate from the edges as well. Secondly the matrix cracks are much more dispersed throughout the laminate in particular cracks in the surface 45° and 90° plies are not local to the hole as in open-hole tests. Another notable difference is the complete absence of delamination which propagates out from the hole in between the parallel matrix cracks of the 0° plies as seen in open-hole tests. Comparing specimen B012 in Fig. 11 to B013 in Fig. 12, it can be seen that the delay in the stiffness loss giving rise to the intermediate plateau at around $E/E_0 = 0.7$, is due to hindrance of the second asymmetric -45/0 delamination from the compressive bolt forces around the hole. This is common for all severities. The damage seen in the other interfaces appear to be similar for both specimens. Using image processing software, bar charts were produced which accurately quantifies the extent of planar delamination areas at each interface through the thickness of the laminate. The 45/90 and 90/-45 interfaces have reached a saturation limit in which the delamination of the -45/0 interface is responsible for the majority of the stiffness degradation.

A single specimen was tested at 50% severity which reached $10^6$ cycles with no measurable stiffness loss (run-out), and was also

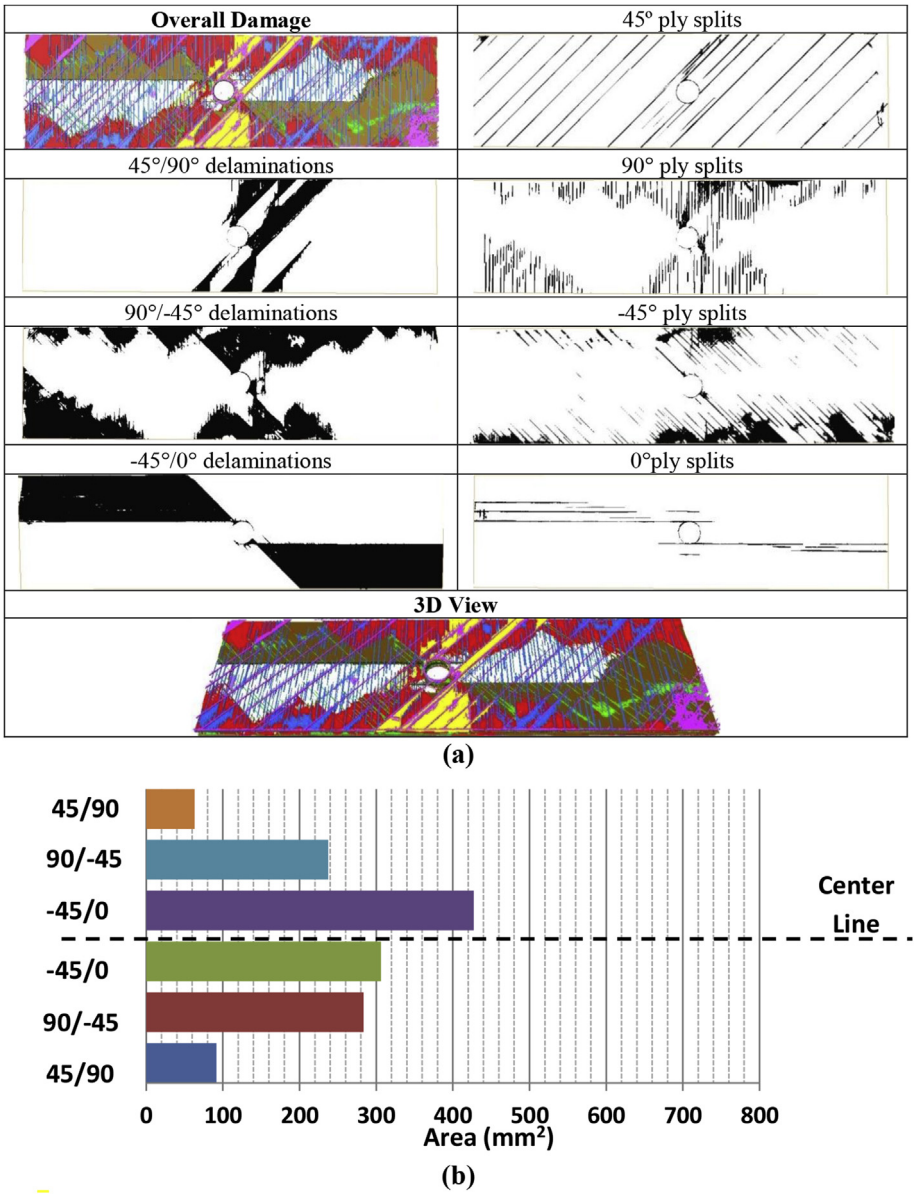


**Fig. 11.** Specimen B012 – 60% severity: (a) CT images, and (b) Damage area quantification through the thickness.

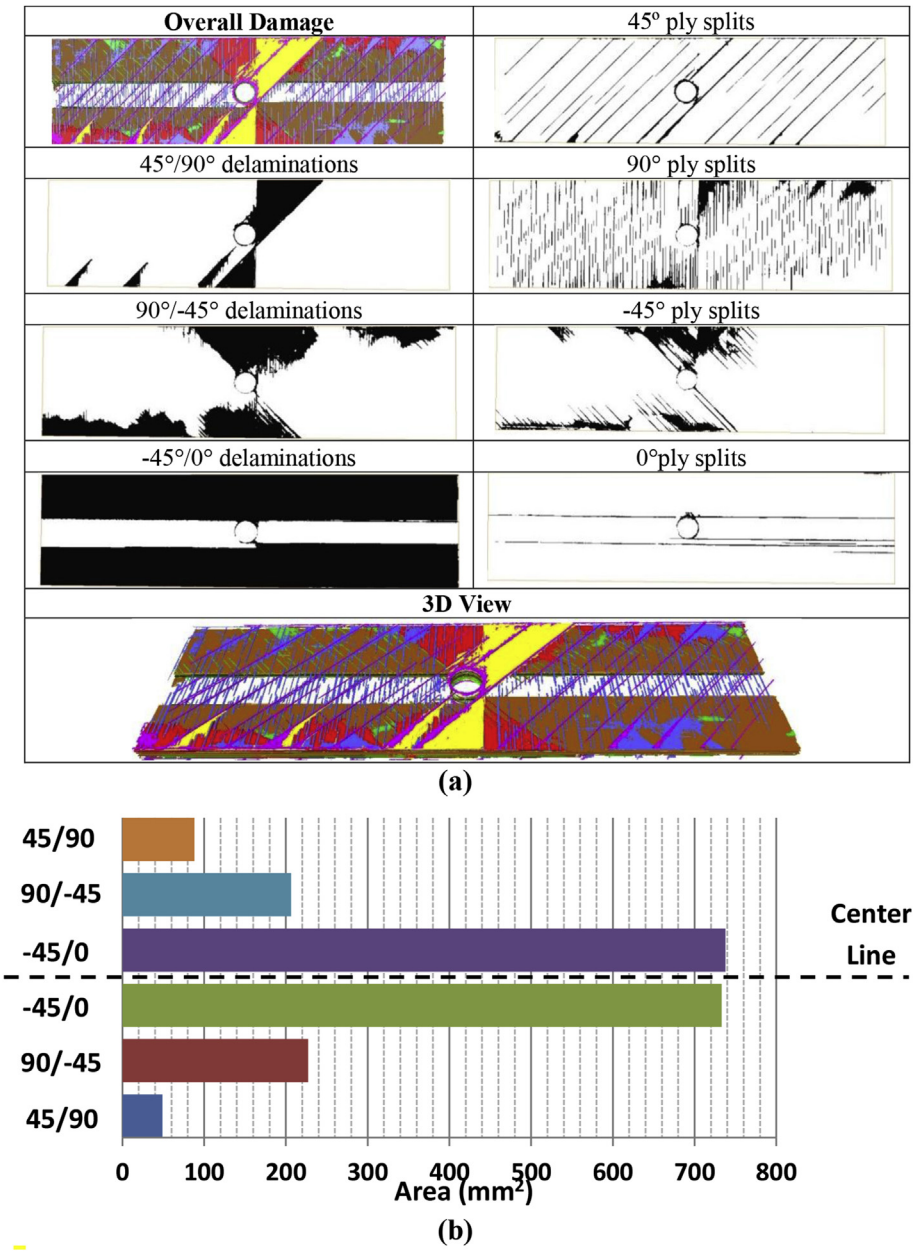


**Fig. 12.** Specimen B013 – 60% severity: (a) CT images, and (b) Damage area quantification through the thickness.

evaluated using X-ray CT. Fig. 13 illustrates the damage in this specimen. The dominant failure process responsible for the majority of the stiffness reduction in failed specimens is the delamination of the -45/0 interface, which is notably absent in this case. There is an extensive amount of matrix cracking throughout the specimen and a significant level of delamination in the 90/-45 interface emanating from the specimen edges. There is a no delamination in the 45/90 interface. Run-outs for the open-hole ply level configuration occurred at 40% severity with much less observable damage [6].

Fig. 14 shows a stiffness curve together with washer pressure for a typical bolt-filled ply-level fatigue test. It shows that there is a similar relationship between the bolt pressure and number of cycles as there is for stiffness loss, and thus the damage of the specimen. The washer pressure drops at around $10^5$ cycles, which implies a loss of integrity of the material beneath it and that damage had initiated around the hole at this point, despite the clamping pressure. The fact that the damage around the hole is coincident with the loss in stiffness suggests that it is the principal failure mode and that the large amount of free-edge delamination seen in the CT scans is secondary.

### 4.2. Bolted hole sublaminate-level fatigue results

The SN curve for the sublaminate bolted hole results (Fig. 15) also shows a substantial increase in the number of cycles to failure in comparison to the open hole specimens for the severities tested. All bolted sublaminate specimens tested failed by pull-out under fatigue loading, whereas for open-hole specimens they failed by delamination in all but the highest severities. The bolt clamp-up thus completely inhibits the delamination failure mode in this case, causing the substantial rise in fatigue life. There is notably less

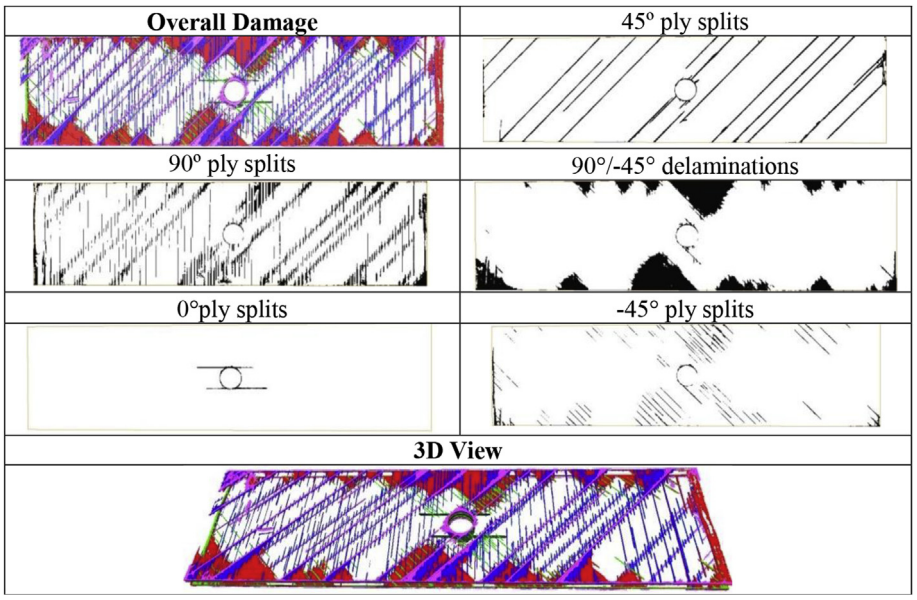


**Fig. 13.** CT images of a runout specimen at 50% severity for a ply-level test at 70 MPa.

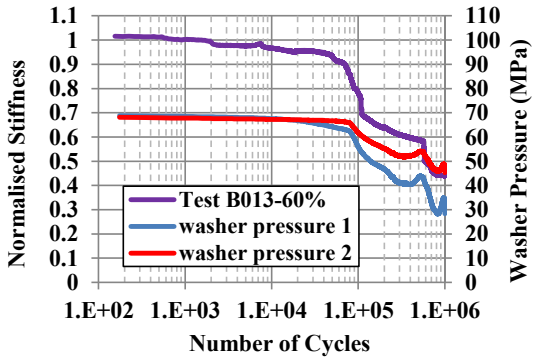


**Fig. 14.** Washer Pressures (primary axis) and stiffness (secondary axis) for the ply-level bolted test B013-60%.

scatter than for the ply-level case as the failure mode is fibre-dominated. Fig. 16(a) and (b) shows the open- and bolted-hole Weibull probability curves respectively. The curve for 85% severity crosses over with the curve for 80% severity, due to an outlier at 85% severity which failed at around 2E4 cycles. The Weibull curves appear to be rather sensitive to scatter and outliers, furthermore they become less reliable for the bolted configurations due to relatively fewer specimens tested in comparison to open-hole configurations.

Although there is a subtle increase in the failure strength in the static case using the higher washer pressure, the effects seen in

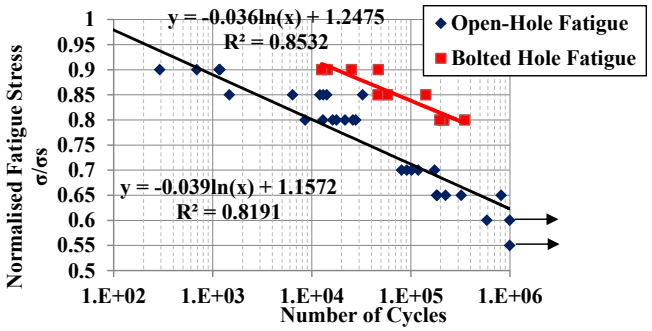


**Fig. 15.** The relationship between open-hole and bolted-hole in fatigue loading for sublaminate-level specimens.

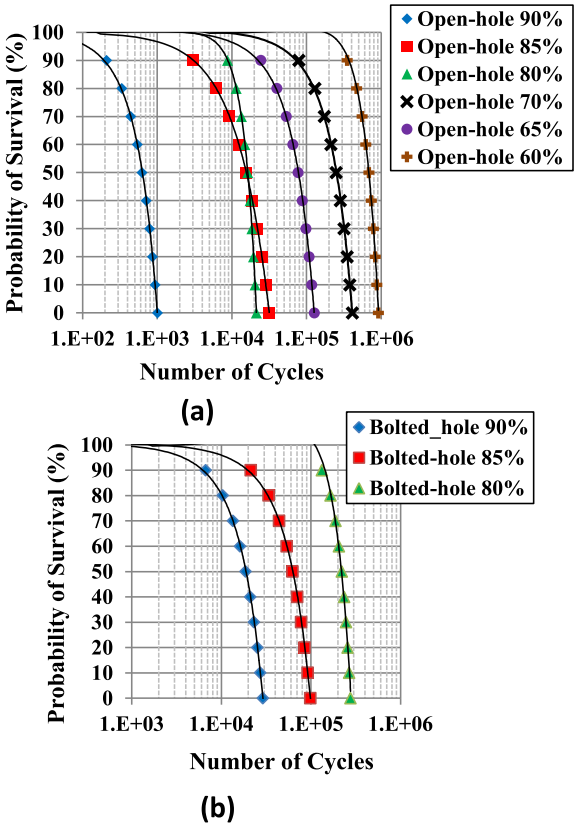


**Fig. 16.** Probability of survival graphs for sublaminate level (a) open- and (b) bolted-hole test programmes.

fatigue are much greater. A plot of normalised stiffness versus number of cycles for a specimen at each severity tested is shown in Fig. 17. In general each test shows a small degradation in the fatigue performance prior to failure by fibre-fracture and pull-out. In each case the failure criterion is met when fibre-failure ensues rather than through gradual stiffness loss prior to pull-out.

Fig. 18 shows a typical relationship between stiffness loss and washer pressure for a bolt-filled fatigue test (sublaminate specimen B010 with an 80% severity). The stiffness gradually degrades as the number of cycles increases from the start of the test until pull-out failure occurs at 213,795 cycles. There is a minor decrease in the washer pressures measured from the compressive strains on both sides of the bush until failure of the specimen. As the specimen fails there is a sharp drop in the washer pressure down to 32 and 36 MPa for washer pressure 1 and 2 respectively. This suggests that there is some damage developing around the clamped hole, as the fatigue test is progressing.

Fig. 19 shows the extent of damage post failure in a test at 80% severity. There is extensive edge delamination at the -45/90 interface but no evidence of damage in the -45/0 interface. The CT slice showing fibre-failure of the central 0° plies is shown without segmentation for clarity.

Fig. 20 shows the extent of zero degree splitting in a typical fatigue failure compared to the quasi-static failure with the same washer pressure of 70 MPa. It shows that the extent of splitting under fatigue loading is much greater for fatigue tests than for quasi-static. The effect of this would be to increase the fatigue life due to the notch blunting further delaying the onset of fibre failure.

## 5. Conclusions

An experimental programme was undertaken to show how damage evolves in bolted composite specimens containing a centrally located hole with a bolted clamping force. This paper shows how the damage mechanisms can change under quasi-static and fatigue loading and how they compare to previous work on specimens containing an open-hole. Also it is shown how the bolted clamping stress inhibits delamination. The enhancement of through-thickness properties is a phenomenon previously reported in the literature, but not extensively for this configuration. The different specimen layups and loading were compared in terms of their overall failure mode and sequence of damage events leading to overall failure. Quasi-static testing of bolted specimens was carried out using two levels of bolt clamping pressures for two different layups. One bolt pressure was chosen for the fatigue study to observe any effects of the through thickness forces on the damage mechanisms and fatigue life. The following points contain some reiteration drawn from previously published material in Ref. [6] which is included for completeness and direct comparison with the bolted testing programme. The key features of the specimen failures can be summarised as follows:-

- The ply level open-hole specimens showed the same overall failure mode of delamination under fatigue and quasi-static tensile loading with run-outs at 40% severity.

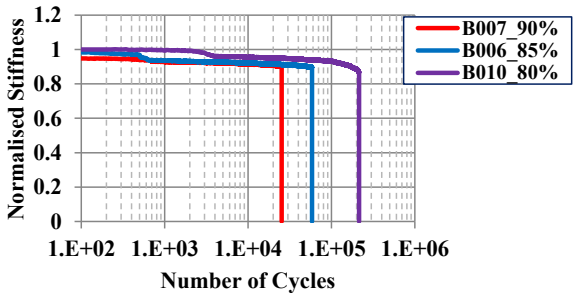


**Fig. 17.** Stiffness loss curve for each of the three severities tested for the bolted sublaminate specimens.

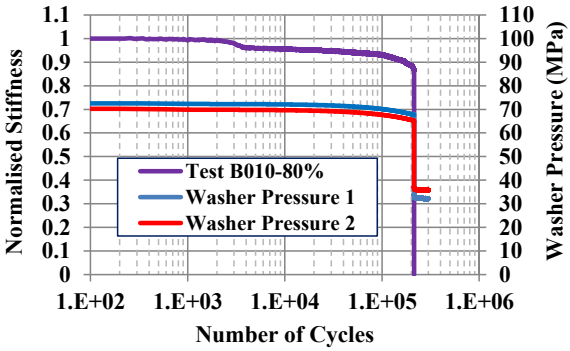


**Fig. 18.** Washer Pressures (primary axis) and stiffness (secondary axis) for the sublaminate-level bolted test B010-80%.

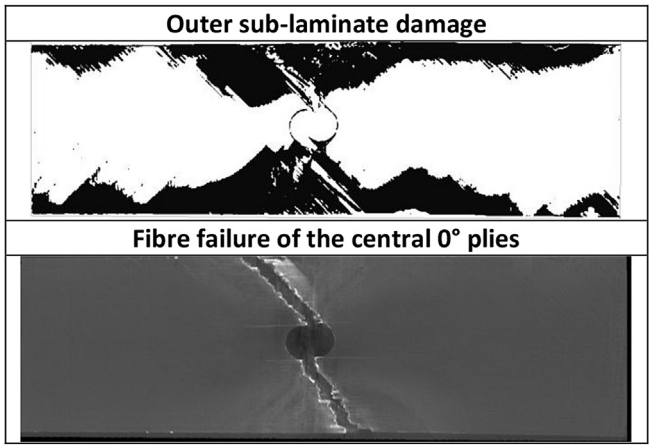


**Fig. 19.** Damage in the surface sublaminate, with the un-segmented image of the central 0 plies showing fibre-failure.

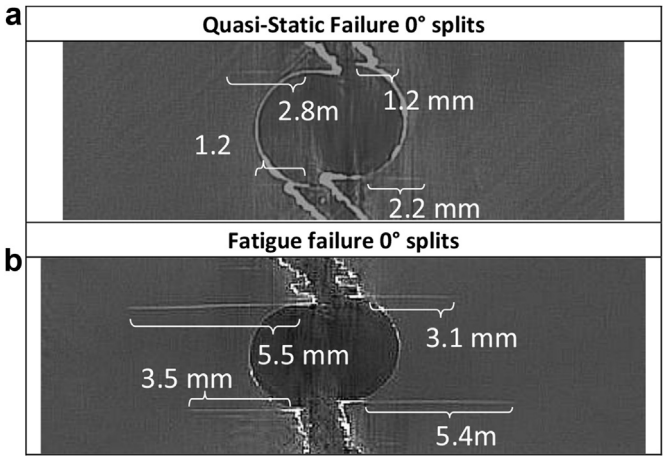


**Fig. 20.** Comparison of zero degree split lengths obtained from CT scans for (a) the static failure, and (b) a typical fatigue failure at 80% severity.

- The sublaminate open-hole specimens showed pull-out failure under quasi-static loading, which changed to overall failure by delamination under fatigue in all but the highest severities with run-outs at 55% severity.
- The ply-level specimens showed the greatest increase in the bolted quasi-static strength for the lower washer pressure of 23 MPa, 3 out of 5 specimens failed by pull-out, and 2 by delamination.
- At the higher washer pressure of 70 MPa, there was a smaller increase in the ply-level quasi-static strength with all specimens failing by pull-out.
- The sublaminate specimens showed only a minor increase in the quasi-static strength under bolted clamping pressures.
- Under fatigue, the ply-level case with a bolt-filled hole showed greater fatigue lives for all severities tested. The through thickness clamping force also delayed the onset of the second asymmetric -45/0 delamination with run-outs at 50% severity.
- The bolted sublaminate case gave greater fatigue lives at each severity tested.
- In all cases the increase in fatigue life was as a result of the clamping stresses delaying the onset or suppressing delamination.

It has been shown in this paper how X-ray CT scanning can be used to provide new information on the detail of damage formation during fatigue loading. This has been used to examine the role of bolt clamp up forces on the damage, in particular delamination. Previous studies have only highlighted the changes of overall strength due to bolting, but here this has been directly related to and explained by the details of the damage formed during both quasi-static and fatigue loading. In the future this information could be used to develop and validate numerical models for prediction of strength and joint performance. Furthermore this paper indicates some of the advantages and disadvantages of using Weibull statistics for sample sizes which are representative of preliminary and exploratory coupon level fatigue testing. The open-hole ply-level configuration gave a good fit of data as the sample size was adequate with consistent failures modes throughout all specimens and severities. The open-hole sublaminate configuration contained fibre dominated failure modes at the highest of severities with delamination dominating severities lower than 85%, which reduces the reliability of the Weibull analysis. For bolted hole configurations a smaller set of data is presented and compared with open-hole data, thus producing more variable Weibull fits.

## Acknowledgements

This work was supported by the Engineering and Physical Sciences Research Council through the EPSRC Centre for Doctoral Training in Advanced Composites for Innovation and Science [grant number EP/G036772/1].

## References

[1] Yan Y, Wen WD, Chang FK, Shyprykevich P. Experimental study on clamping effects on the tensile strength of composite plates with a bolt-filled hole. Compos Part A: Appl Sci Manuf 1999;30(10):1215–29.
[2] Schön J, Nyman T. Spectrum fatigue of composite bolted joints. Int J Fatigue 2002;24(2–4):273–9.
[3] Persson E, Eriksson I. Fatigue of multiple-row bolted joints in carbon/epoxy laminates: ranking of factors affecting strength and fatigue life. Int J Fatigue 1999;21(4):337–53.
[4] Starikov R, Schön J. Local fatigue behaviour of CFRP bolted joints. Compos Sci Technol 2002;62(2):243–53.
[5] Green BG, Wisnom MR, Hallett SR. An experimental investigation into the tensile strength scaling of notched composites. Compos Part A-Appl Sci Manuf 2007;38(3):867–78.
[6] Nixon-Pearson OJ, Hallett SR, Withers PJ, Rouse J. Damage development in open-hole composite specimens in fatigue. Part 1: experimental investigation. Compos Struct 2013;106(December):882–9.
[7] Nixon-Pearson OJ, Hallett SR, Harper PW, Kawashita LF. Damage development in open-hole composite specimens in fatigue. Part 2: numerical modelling. Compos Struct 2013;106(December):890–8.
[8] Nixon-Pearson OJ, Hallett SR. An investigation into the damage development and residual strengths of open-hole specimens in fatigue. Compos Part A: Appl Sci Manuf 2015;69(0):266–78.
[9] Spearing SM, Beaumont PWR, Kortschot MT. The fatigue damage mechanics of notched carbon-fiber PEEK laminates. Composites 1992;23(5):305–11.
[10] Mohlin T, Carlsson L, Blom AF. An X-ray radiography study of delamination growth in notched carbon/epoxy laminates. In: Proceedings of testing, evaluation and quality control of composites. Guildford, England; 1983. p. 85–92.
[11] Mohlin T, Blom AF, Carlsson L, Gustavsson AI. Delamination growth in notched graphite/epoxy laminates under compression fatigue loading. ASTM STP 876. In: Johnson WS, editor. Delamination and debonding of materials; 1985. p. 168–88.
[12] Scott AE, Mavrogordato M, Wright P, Sinclair I, Spearing SM. In situ fibre fracture measurement in carbon-epoxy laminates using high resolution computed tomography. Compos Sci Technol 2011;71(12):1471–7.
[13] Moffat AJ, Wright P, Buffiere JY, Sinclair I, Spearing SM. Micromechanisms of damage in 0 degrees splits in a [90/0](s) composite material using synchrotron radiation computed tomography. Scr Mater 2008;59(10):1043–6.
[14] Nixon-Pearson OJ, Hallett S. An investigation into the damage development and residual strengths of open-hole specimens in fatigue. In: Proceedings of the International Conference on composite materials ICCM19. Montreal; 2013.
[15] Hexcel 8552, Epoxy matrix product datasheet. Pdf download from: www.hexcelcomposites.com/Markets/Products/Prepreg/PrepregDownld.html.
[16] Hallett SR, Green BG, Jiang WG, Wisnom MR. An experimental and numerical investigation into the damage mechanisms in notched composites. Compos Part A 2009;40(5):613–24.
[17] Mall S, Weidenaar WA. Tension-compression fatigue behaviour of fibre-reinforced ceramic matrix composite with circular hole. Composites 1995;26(9):631–6.
[18] Withers PJ, Preuss M. Fatigue and damage in structural materials studied by X-ray tomography. Annu Rev Mater Res 2012;42:81–103.
[19] Wright P, Moffat A, Sinclair I, Spearing SM. High resolution tomographic imaging and modelling of notch tip damage in a laminated composite. Compos Sci Technol 2010;70(10):1444–52.
[20] Sakin R, Ay İ. Statistical analysis of bending fatigue life data using Weibull distribution in glass-fiber reinforced polyester composites. Mater Des 2008;29(6):1170–81.
[21] ASTM. Standard practice for statistical analysis of linear or linearized stress-life (S-N) and strain-life fatigue data. 2010.